Supporting Information

Highly sensitive detection of microcystin-LR under visible light by self-powered photoelectrochemical aptasensor based on CoO/Au/g-C_3N_4 Z-scheme heterojunction

Lin Tang[a,b*], Xilian Ouyang[a,b], Bo Peng[a,b], Guangming Zeng[a,b*], Yuan Zhu[a,b], Jiangfang Yu[a,b], Chengyang Feng[a,b] Siyuan Fang[a,b], Xu Zhu[a,b], Jisui Tan[a,b],

[a]College of Environmental Science and Engineering, Hunan University, Changsha 410082, China

[b]Key Laboratory of Environmental Biology and Pollution Control (Hunan University), Ministry of Education, Changsha 410082, Hunan, China[1]

[*]Corresponding author: Tel.:+86-731-88822778; Fax.: +86-731-88822778

E-mail: tanglin@hnu.edu.cn (L. Tang), zgming@hnu.edu.cn (G.M. Zeng).

1. Materials and apparatus

Tripolycyanamide, cobalt acetate ($Co(CH_3COO)_2•4H_2O$), ethanol, n-octanol, Ethylenediaminetetraacetic acid (EDTA), and Nafion (5 wt%) were purchased from Sinopharm Chemical Reagent Co., Ltd (Shanghai, China). Tris (2-carboxyethyl) phosphine (TCEP), 6-Mercaptohexanol (MCH), tris (hydroxymethyl) aminomethane (Tris) were purchased from Sigma-Aldrich (St. Louis, MO, USA). All chemicals were of analytical grade and were used without further purification. Microcystin-LA (MC-LA), microcystin-YR (MC-YR), and microcystin-LR (MC-LR) were obtained from J&K Chemical Ltd. (Beijing, China). The high-performance liquid chromatography-purified Single-stranded DNA (ssDNA) aptamer for MC-LR used in this work was synthesized by Sangon (Shanghai, China) with the following sequences: 5'-SH-GGC GCC AAA CAG GAC CAC CAT GAC AAT TAC CCA TAC CAC CTC ATT ATG CCC CAT CTC CGC-3'.

Standard microcystin samples was dissolved in binding buffer (50 mM Tris-HCl buffer. pH 7.4, which contained 0.1 mM NaCl, 5mM $MgCl_2$, 0.2 M KCl, 1.0 mM EDTA) to obtain various concentrations of microcystin. Wash buffer solution was10 mM Tris-HCl buffer solution (pH 7.4) containing 0.2 M NaCl (TBS). The ssDNA aptamer solution was prepared by dissolving ssDNA in the binding buffer containing 0.1 mM TCEP. Phosphate buffer solution (PBS) (0.1 M pH 7.4) containing 0.1 M KCl was used as the supporting electrolyte. All solutions were prepared with ultrapure water (18.25 MΩ cm) purified by a Milli-QTM system (Millipore).

The transmission electron microscopy (TEM), high resolution transmission electron microscope (HRTEM) and high-angle annular dark-field scanning transmission electron microscopy (HAADF-STEM) were obtained by a Tecnai G2 F20 S-TWIX electron microscope (FEI, Holland). Fourier transform infrared (FT-IR) spectra were obtained on an IRAffinity-1 Fourier transform infrared spectrometer (Shimadzu, Japan) at room temperature by the standard KBr disk method. The photoluminescence (PL) spectra were obtained by a F-7000 fluorescence spectrometer, and the Ultraviolet visible (UV-vis) spectrum was recorded by a UV

spectrophotometer (Hitachi U4100 UV Spectrometer). An X-ray photoelectron spectroscopy (Thermo Fisher ESCALANB 250Xi), a Model CS501-SP thermostat (Huida Instrument, Chongqing, China), an X-ray diffractometer (XRD) (Bruker AXS D8 Advances) at a scan rate (2θ) of $0.05°s^{-1}$ with Cu Kα irradiation source were used in this work. A 300 W Xe lamp (PLS/SXE 300C, Beijing Perfect light Co.,Ltd) was used as the irradiation source to produce visible-light. The high-performance liquid chromatography system equipped with an ultraviolet detector (Agilent USA) was used to detect MC-LR in comparative experiment. All electrochemical and photoelectrochemical measurements were conducted on CHI760D electrochemical workstation (Chenhua Instrument, Shanghai, China). The conventional three-electrode system used in this work was composed of a modified ITO slice as the working electrode, a saturated calomel electrode (SCE) as the reference electrode and a Pt foil as the counter electrode. A model pHSJ-3 digital acidimeter (Shanghai Leici Factory China) was used for solution pH measurement. A Sigma 1-14 Micro centrifuge (Sigma, Germany), a Sigma 4K15 laboratory centrifuge, a vacuum freezing dryer and a mechanical vibrator were used in this work. All the work was conducted at room temperature (25°C) unless otherwise mentioned.

2. The synthesis of g-C_3N_4 and CoO/g-C_3N_4 composite

Typically, 6 g of tripolycyanamide was heated at 550 °C for 4 h in static air with a ramp rate of 2.3 °C/min. Then 1.5 g of the bulk g-C_3N_4 obtained above was milled and heated at 500 °C for 2 h with a ramp rate of 2.3 °C/min. The ultimately obtained white powder was the g-C_3N_4 nanosheets.

CoO/g-C_3N_4 composite with different mass of CoO (10 wt.%, 20 wt.%, 30 wt.%, 40 wt.%, 50 wt.%, 60 wt.%, 70 wt.%) were synthesized according to the reported previously [1], with slight modification, 0.25 g prepared g-C_3N_4 was dispersed in a mixture of 16 mL of ethanol and 4 mL n-octanol and stirred for 1 h to form a homogeneous solution, then a suitable amount of $Co(CH_3COO)_2 \cdot 4H_2O$ was added with continuous stirring for 2 h. The obtained fuchsia mixture was heated at 220 °C for 4 h. After cooling down to room temperature, the obtained powders were washed three times with ethanol and finally dried at 70 °C in an oven. Pure CoO nanoparticles were fabricated by the similar processes without the addition of g-C_3N_4.

3. *Photo-deposition of Ag Nanoparticles*

According to the previous report[2], the photo-deposition of Ag NPs can be achieved with $AgNO_3$ as the precursor. Typically, an appropriate amount of $AgNO_3$ (20 mg/mL) and the CoO/Au/g-C_3N_4 composites were added to 80 mL of methanol aqueous solution (20 wt%), and then, the suspension was irradiated by a 300 W Xe lamp under a constant stirring for 1 h. After that, the suspension was thoroughly washed with deionized water and ethanol several times. Then the achieved sediment was dried at 60 ℃ for 8 h in a vacuum oven. The prepared samples were marked as Ag/CoO/Au/g-C_3N_4.

4. Real sample preparation

The lake water samples were obtained from Taozi Lake (TLW) and Dongting Lake (DLW) when the cyanophyta bloom. Some tap water samples (TW) were also collected. The sampling sites were shown in Fig. S5. The original water samples were filtered with 0.45 μm membrane to remove large suspended particles and microorganisms, and the pH was adjusted to 7.4 with PBS before the detection with the well-established PEC aptasensor. For the high-performance liquid chromatography-ultraviolet (HPLC-UV) measurement, the samples were pretreated according to the standards of China (GB/T 20466-2006). Firstly, the samples were treated with a 0.22 μm syringe filter to remove large suspended particles and microorganisms, and then, the pH was adjusted to 7.4 with PBS for detection. In order to test the sensor in detection of MC-LR at high level, the selected samples were also spiked with MC-LR standards to obtain higher concentrations. Next, the samples were passed through a preprocessed SPE column at a flow rate of 5 mL/min, and each SPE column was rinsed by 10 mL purewater and 10 mL 20% methanol. In order to remove residual moisture, the analytes were eluted with 10 mL 0.1 % trifluoroacetic acid methanol solution, and then concentrated to less than 1 mL with pure nitrogen. Finally, the obtained water samples were dissolved by 50% methanol to make up to 1 mL [3]. Before analysis, the water samples were stored at 4°C in the dark.

5. *EDX data*

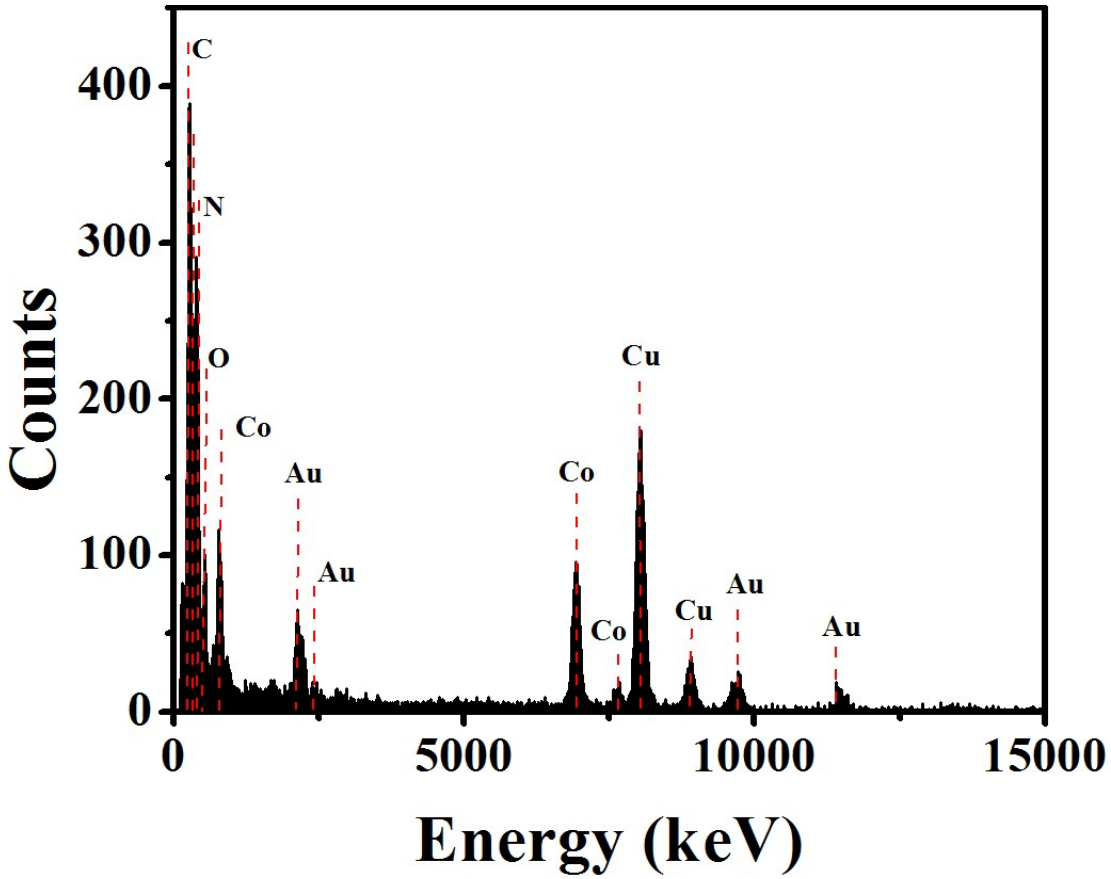

Fig. S1. EDX spectra of CoO/Au/g-C_3N_4 composite.

6. *The confirmation of Z-scheme system*

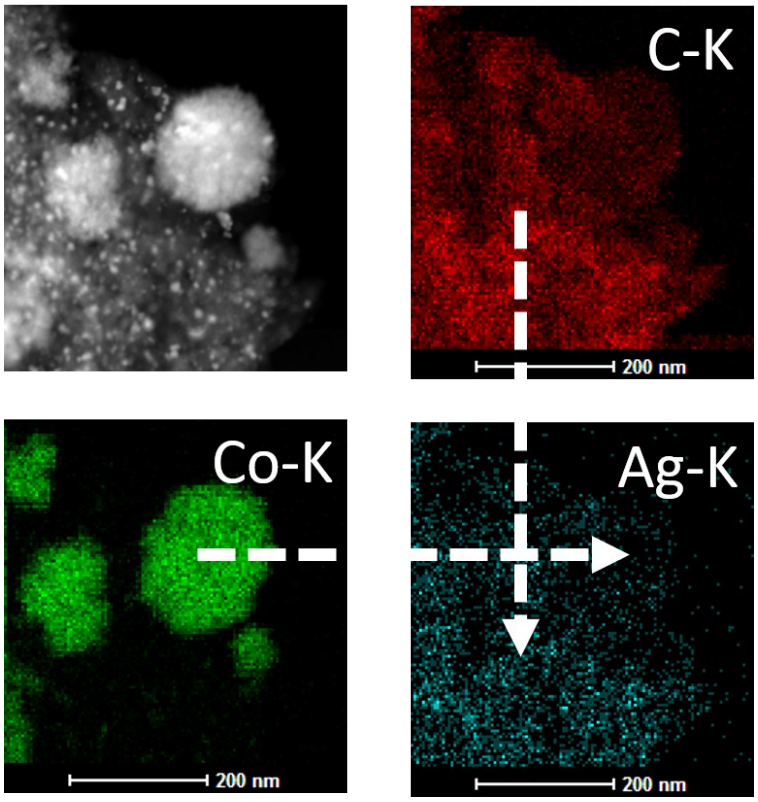

Fig. S2 HAADF-STEM image and corresponding mapping images for the Ag/CoO/Au/g-C_3N_4 composites

In this designed Z-scheme system, The Au NPs play the role as a suitable electron media to remain the stronger reducibility and oxidizability on different active sites and to promote the separation efficiency of the photoinduced electron-hole pairs. [4]. In this work, we qualitatively confirmed the transfer direction of electrons by reducing of $AgNO_3$ on the surface of CoO/Au/g-C_3N_4 composites. The aggregated location of photogenerated electron in this system can be determined through the Ag NPs reduction deposition site, so as to confirm the path of electron transfer. Fig S2 shows that the mapping images of Ag-K was similar to that of C-K, indicating that Ag were mainly deposited on the surface of g-C_3N_4 instead of CoO[5]. The results verified that the photoinduced electrons were accumulated in g-C_3N_4[6]. The formation of Z-scheme system is further proved.

7. XPS data

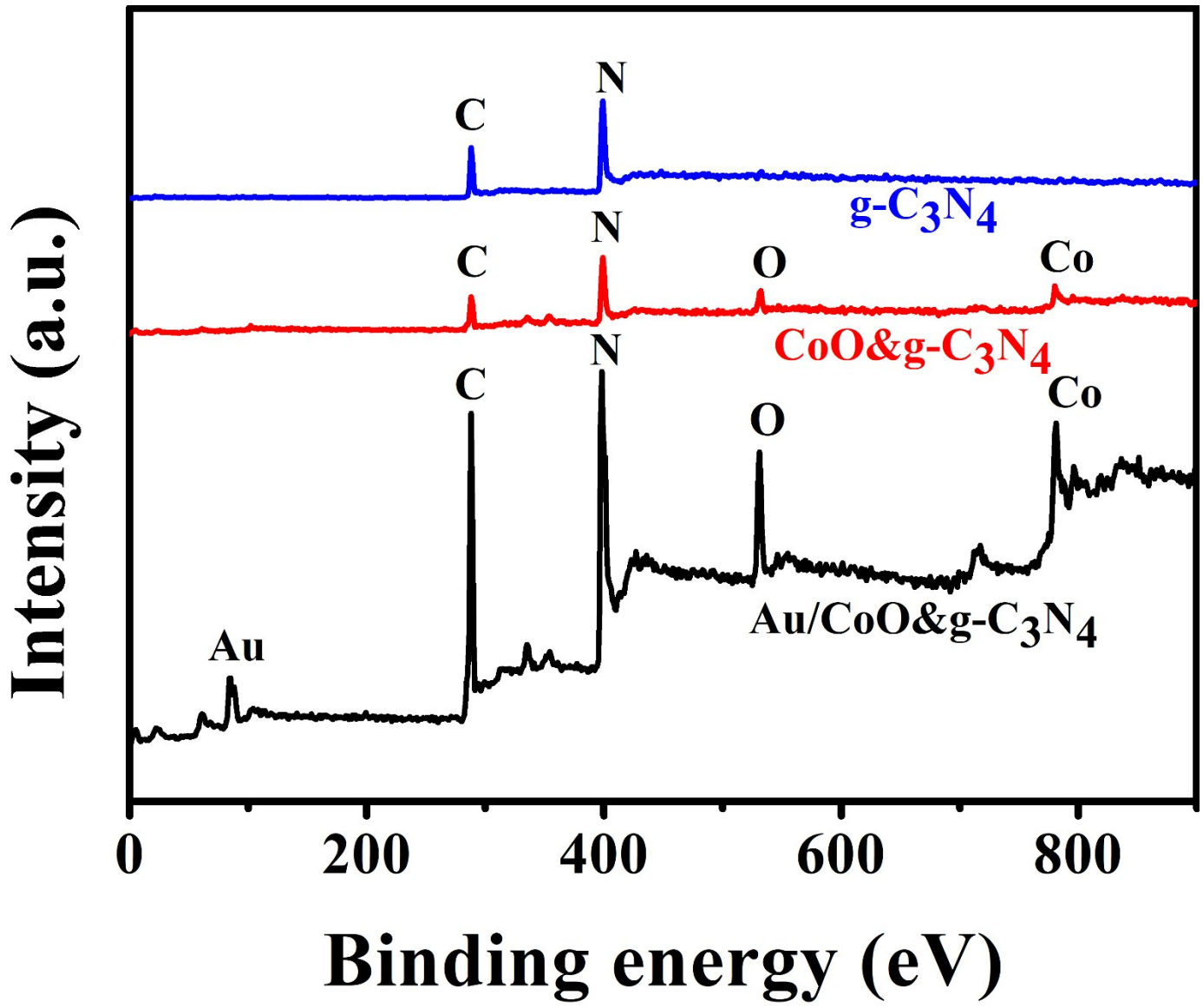

Fig. S3. Full-scan XPS spectrum of CoO; CoO/g-C_3N_4 and CoO/Au/g-C_3N_4 composite.

8. *Optimization of experimental conditions*

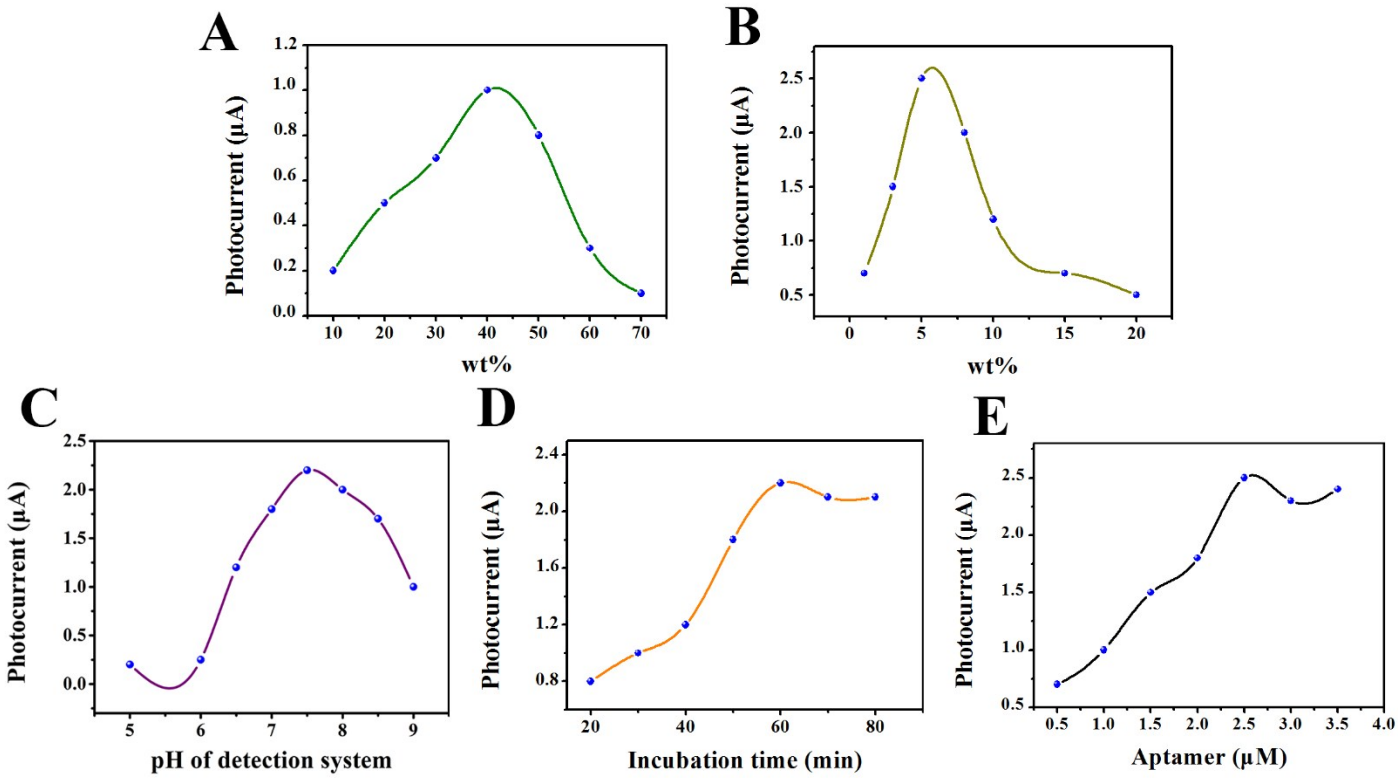

Fig. S4. Effects of (A) CoO wt% in CoO/Au/g-C_3N_4; (B) Au wt% in CoO/Au/g-C_3N_4; (C) the pH value of detection solution; (D) incubation time with MC-LR (1 pM) and (E) concentration of MC-LR aptamer in 0.1 M PBS (pH 7.4) containing 0.1 M Na_2SO_4.

In this study, the concentration of CoO varied from 10 wt.% to 70 wt.%. In Fig. S3A, the photocurrent of CoO/g-C_3N_4/ITO electrode significantly increased with increase in concentration of CoO from 10 wt.% to 40 wt.%, illustrating that more CoO/g-C_3N_4 composite could provide more photogenerated holes and electrons to participate in the PEC process. When the concentration of CoO exceeds 70 wt.%, the photocurrent decreases. Thus, 40 wt.% CoO/g-C_3N_4 was used for fabricating the PEC sensor. Furthermore, the concentration of Au NPs has an important influence on the photocurrent responses. As shown in Fig. S3B, it was found that the photocurrent value was maximum when the concentration at 5 wt.%. Thus, the concentration of 5 wt.% was adopted as the optimal concentration of Au NPs.

The pH value of buffer solution was also investigated for PEC aptamer sensor. One can see from Fig. S3C, the maximum photocurrent responses was obtained at pH 7.4. Thus, pH 7.4 was used in the detection for MC-LR. Incubation time on the response of the electrode is another influential parameter. It can be

observed from Fig. S3D, that the photocurrent response toward MC-LR increases with the incubation time increased, which can be ascribed to that long incubation time can increase the amount of MC-LR molecules captured by the aptamers. When the incubation time was longer than 60 min, the curve tended to a stable value, demonstrating binding interaction with the MC-LR molecules reached saturation. Consequently, 60 min was chosen as the incubation time for PEC detection.

Because of the specific interaction between the aptamer and MC-LR molecules, the concentration of the aptamer plays an important role in optimizing the photocurrent signal. From Fig. S3E, after incubated with 1 pM MC-LR, there was a gradual increase in photocurrent intensity with increase in the aptamer concentration from 0.5 to 2.5 μM. However, photocurrent intensity decreased when the aptamer concentration exceeded 2.5 μM, which could be attributed to that the increased steric hindrance impeded the transfer of electrons. As a result, 2.5 μM was chosen as the optimal concentration of aptamer in this experiment.

9. *The sampling sites of natural water sources*

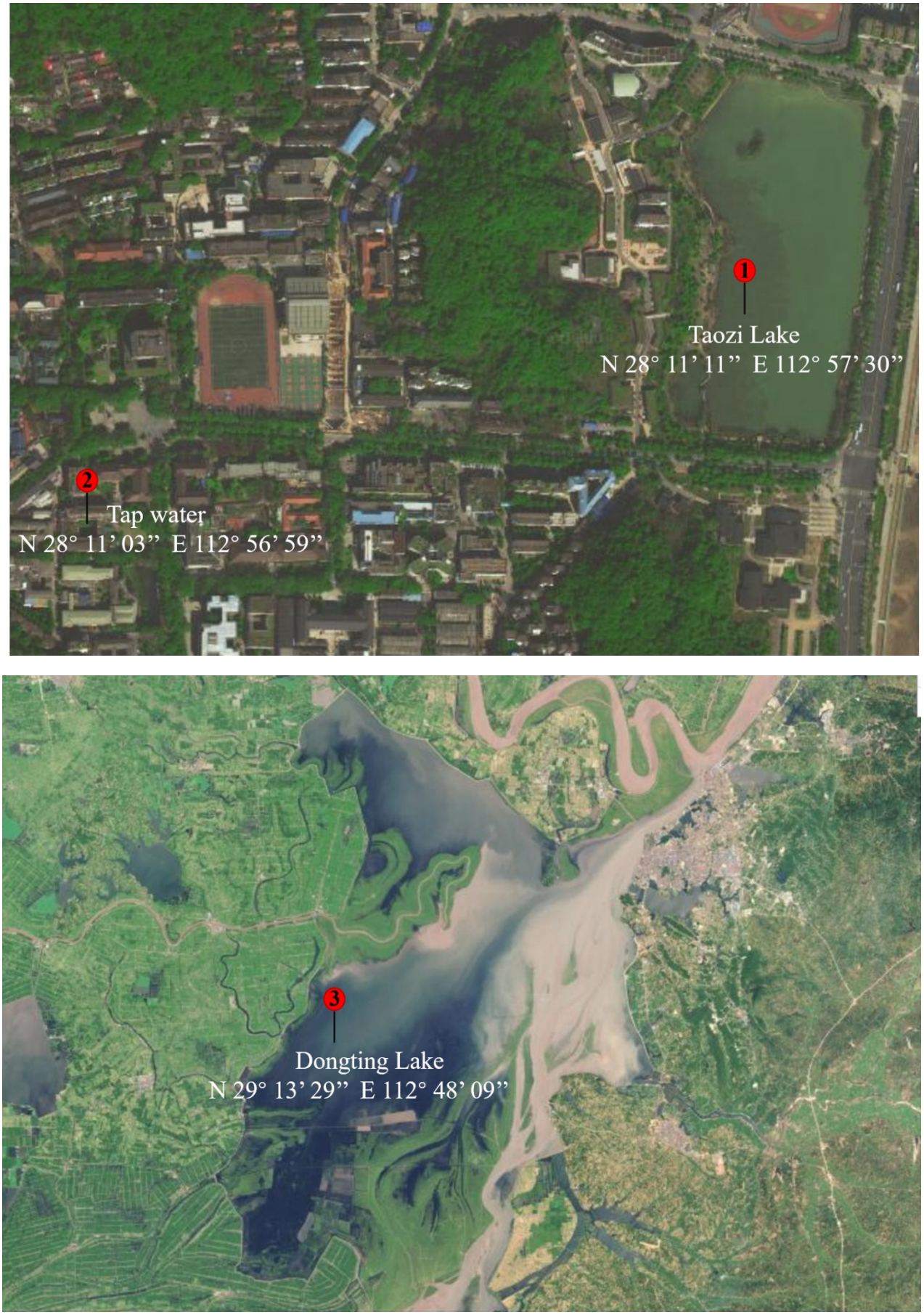

Fig. S5. The sampling sites of natural water sources, 1, Taozi Lake; 2, Tap water; 3, Dongting Lake.

10. Long term stability

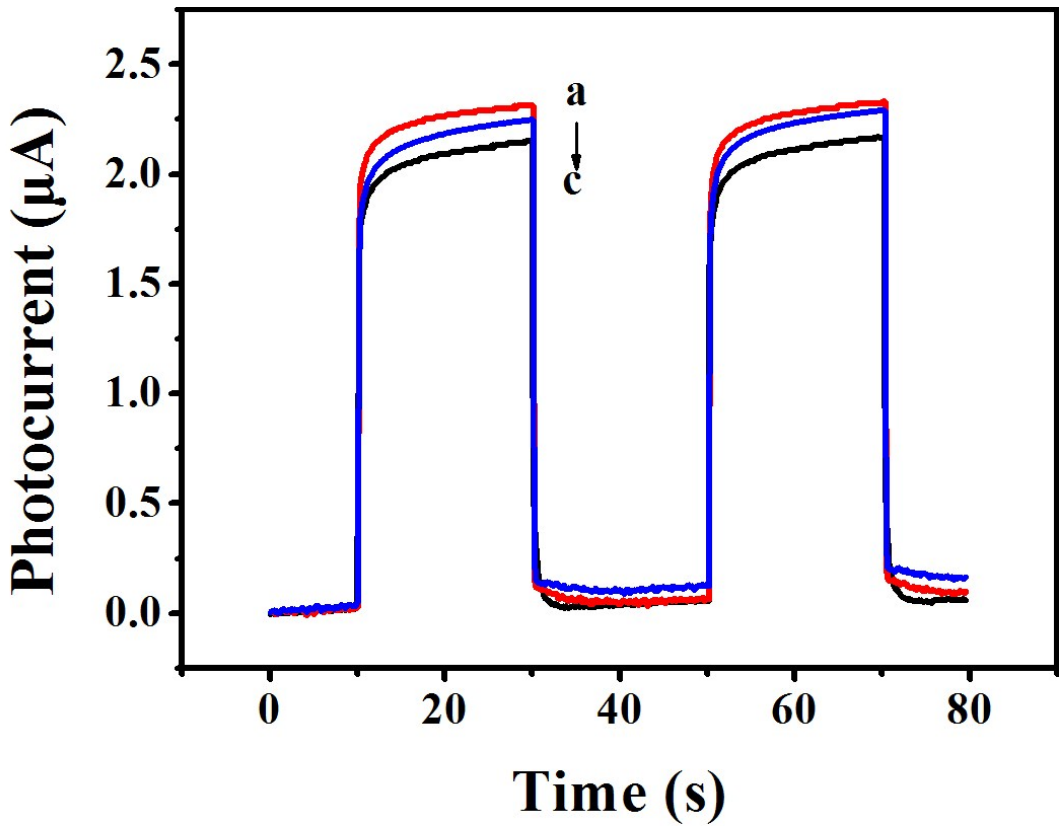

Fig.S6. The long term stability of the prepared PEC aptasensor after storage of (a) the present (b)1 month and (c) 3 months

.

11. Comparisons of prepared PEC aptasensor with other reported works

Table S1 Comparison of availible published sensors for analysis of MC-LR

Methods	LOD	Analytical range	Ref.
CdS/TiO_2 nanorod arrays based on PEC immunosensor	1 pM	5 pM-500 nM	[7]
A Multiwalled-carbon-nanotube-based biosensor	40 pM	50 pM-20 nM	[8]
PEC sensor based on CdS/Fe_2O_3 co-sensitized TiO_2 nanorod arrays	0.3 pM	0.5 pM-100nM	[9]
An electrochemical immunosensor based on G-quadruplex/hemin	0.3 pM	0.5 pM-25 nM	[10]
A single-walled carbon nanotube-based label-free	0.6 pM	1 pM-1000 pM	[11]
A fluorescence aptasensor based on MoS_2	2 pM	10 pM-50 nM	[12]
An aptamer-based colorimetric sensor	0.37 nM	0.5 nM-7.5 nM	[13]
A PEC aptasensor based on $CoO/Au/g\text{-}C_3N_4$ Z scheme heterojunction	0.01 pM	0.1 pM-10 nM	This work

References

1. F. Guo, W. Shi, C. Zhu, H. Li and Z. Kang, *Appl. Catal., B* 2018, **226**, 412-420.
2. L. Mu, Y. Zhao, A. Li, S. Wang, Z. Wang, J. Yang, Y. Wang, T. Liu, R. Chen, J. Zhu, F. Fan, R. Li and C. Li, *Energy Environ. Sci*, 2016, **9**, 2463-2469.
3. L. Hou, Y. Ding, L. Zhang, Y. Guo, M. Li, Z. Chen and X. Wu, *Sens. Actuators, B*, 2016, **233**, 63-70.
4. H. Li, W. Tu, Y. Zhou and Z. Zou, *Advanced Science*, 2016, **3**.
5. Y. Si, S. Cao, Z. Wu, Y. Ji, Y. Mi, X. Wu, X. Liu and L. Piao, *Nano Energy*, 2017, **41**, 488-493.
6. C. Liu, H. Huang, L. Ye, S. Yu, N. Tian, X. Du, T. Zhang and Y. Zhang, *Nano Energy*, 2017, **41**, 738-748.
7. J. Wei, A. Qileng, Y. Yan, H. Lei, S. Zhang, W. Liu and Y. Liu, *Anal. Chim. Acta* 2017, **994**, 82-91.
8. C. Han, A. Doepke, W. Cho, V. Likodimos, A. A. de la Cruz, T. Back, W. R. Heineman, H. B. Halsall, V. N. Shanov, M. J. Schulz, P. Falaras and D. D. Dionysiou, *Adv. Funct. Mater.* 2013, **23**, 1807-1816.
9. J. Wei, X. Xie, W. Chang, Z. Yang and Y. Liu, *Sens. Actuators, B,* 2018, **276**, 180-188.
10. C. Gan, B. Wang, J. Huang, A. Qileng, Z. He, H. Lei, W. Liu and Y. Liu, *Biosens. Bioelectron.* 2017, **98**, 126-133.
11. F. Tan, N. M. Saucedo, P. Ramnani and A. Mulchandani, *Environ. Sci. Technol.*, 2015, **49**, 9256-9263.
12. J. Lv, S. Zhao, S. Wu and Z. Wang, *Biosens. Bioelectron.* 2017, **90**, 203-209.
13. X. Li, R. Cheng, H. Shi, B. Tang, H. Xiao and G. Zhao, *J. Hazard. Mater.* 2016, **304**, 474-480.